# UNCLASSIFIED

| AD NUMBER |
|---|
| ADB008821 |
| **LIMITATION CHANGES** |

TO:

Approved for public release; distribution is unlimited.

FROM:

Distribution authorized to U.S. Gov't. agencies only; Test and Evaluation; DEC 1975. Other requests shall be referred to U.S. Army Ballistic Research Laboratories, Attn: AMXBR-SS, Aberdeen Proving Ground, MD 21005.

| AUTHORITY |
|---|
| USAARDC ltr, 8 Mar 1978 |

## THIS PAGE IS UNCLASSIFIED

THIS REPORT HAS BEEN DELIMITED
AND CLEARED FOR PUBLIC RELEASE
UNDER DOD DIRECTIVE 5200.20 AND
NO RESTRICTIONS ARE IMPOSED UPON
ITS USE AND DISCLOSURE.

DISTRIBUTION STATEMENT A

APPROVED FOR PUBLIC RELEASE;
DISTRIBUTION UNLIMITED.

AD

# BRL

MEMORANDUM REPORT NO. 2573

THREE-DIMENSIONAL BOUNDARY LAYER RESEARCH
AS APPLIED TO THE MAGNUS EFFECT ON SPINNING
PROJECTILES

D D C

JAN 29 1976

A

Walter B. Sturek

December 1975

USA BALLISTIC RESEARCH LABORATORIES
ABERDEEN PROVING GROUND, MARYLAND

| REPORT DOCUMENTATION PAGE | READ INSTRUCTIONS BEFORE COMPLETING FORM |
|---|---|

| 1. REPORT NUMBER | 2. GOVT ACCESSION NO. | 3. RECIPIENT'S CATALOG NUMBER |
|---|---|---|
| BRL Memorandum Report No. 2573 | BRL-MR-2573 | |

**4. TITLE (and Subtitle)**
THREE-DIMENSIONAL BOUNDARY LAYER RESEARCH AS APPLIED TO THE MAGNUS EFFECT ON SPINNING PROJECTILES

**5. TYPE OF REPORT & PERIOD COVERED**
Final rept.

**6. PERFORMING ORG. REPORT NUMBER**

**7. AUTHOR(s)**
Walter B. Sturek

**8. CONTRACT OR GRANT NUMBER(s)**
29 P.

**9. PERFORMING ORGANIZATION NAME AND ADDRESS**
U.S. Army Ballistic Research Laboratories
Aberdeen Proving Ground, Maryland 21005

**10. PROGRAM ELEMENT, PROJECT, TASK AREA & WORK UNIT NUMBERS**
RDT&E-1T161102A33H

**11. CONTROLLING OFFICE NAME AND ADDRESS**
U.S. Army Materiel Command
5001 Eisenhower Avenue
Alexandria, Virginia 22333

**12. REPORT DATE**
DECEMBER 1975

**13. NUMBER OF PAGES**
32

**14. MONITORING AGENCY NAME & ADDRESS(if different from Controlling Office)**

**15. SECURITY CLASS. (of this report)**
UNCLASSIFIED

**15a. DECLASSIFICATION/DOWNGRADING SCHEDULE**

**16. DISTRIBUTION STATEMENT (of this Report)**

Distribution limited to US Government agencies only; Test and Evaluation; December 1975. Other requests for this document must be referred to Director, USA Ballistic Research Laboratories, ATTN: AMXBR-SS, Aberdeen Proving Ground, Maryland 21005.

**17. DISTRIBUTION STATEMENT (of the abstract entered in Block 20, if different from Report)**

**18. SUPPLEMENTARY NOTES**

**19. KEY WORDS (Continue on reverse side if necessary and identify by block number)**

Numerical Computations
Magnus
Three-Dimensional Turbulent Boundary Layer
Boundary Layer on Spinning Body of Revolution
Inviscid Flow Computations
Laminar Boundary Layer
Wall Static Pressure

**20. ABSTRACT (Continue on reverse side if necessary and identify by block number)** (1ca)

Due to Army interest in predicting Magnus effects on artillery projectiles, the Ballistic Research Laboratories are carrying out experimental and theoretical research studies of the boundary layer on yawed, spinning bodies of revolution in supersonic flow. In this paper, computed results are shown for circumferential velocity profiles and boundary layer displacement thickness for the laminar boundary layer on a yawed, spinning cone. A comparison between computed values and experimental strain gage balance measurements of Magnus force is
(Continued)

DD FORM 1473 EDITION OF 1 NOV 65 IS OBSOLETE

050 750

20. ABSTRACT (Continued):

shown to yield encouraging agreement. Surveys of the boundary layer on a yawed, spinning tangent-ogive-cylinder model have been made at azimuthal stations completely about the circumference of the model. Measurements have also been made of wall static pressure on a yawed body of revolution. Examples of these data are discussed.

# TABLE OF CONTENTS

3

LIST OF ILLUSTRATIONS

## I.  INTRODUCTION

Recent Army interest in obtaining increased range and greater pay-load capacity in artillery projectiles has led to designs with long, slender ogives, increased projectile length, and boattailed afterbodies. These designs have resulted in decreased drag with a resulting increase in range; however, the aerodynamic stability of these shapes is less than more conventional designs.  This means that these new shapes are more sensitive to a Magnus induced instability.  As a result, the Army has increased its research effort to develop a method for computing Magnus effects that will be useful in artillery projectile design.

As shown in Figure 1, the Magnus force is a side force that occurs on a spinning projectile in flight at angle-of-attack.  Magnus is a small force, it is typically 1/10 to 1/100 of the normal force; however, its effect is important because the Magnus moment acts to undamp the projectile throughout its flight.

Magnus has been modeled theoretically as resulting from spin induced distortion of the boundary layer.  This effect is illustrated schematically in Figure 2 where a cross-sectional view of a body of revolution is shown.  The body is at angle of attack as indicated by the cross flow velocity.  In the view where there is no surface spin, the profile of the edge of the boundary layer is symmetric with respect to the plane of the angle of attack.  In the view where the surface is spinning, the profile of the boundary layer is asymmetric with respect to the plane of the angle of attack--thus, the inviscid pressure distribution is asymmetric and yields a net side force.

## II.  COMPUTATIONS OF THE MAGNUS EFFECT

Since the Magnus effect is a viscous phenomenon, the computation of the boundary layer is the foundation for computations of the Magnus force.  The boundary layer we are considering is fully three-dimensional with the added complication of the interaction of surface spin with the cross flow velocity.  The inviscid flow also requires special attention since, in order to compute the Magnus force, the inviscid flow program must be able to compute the three-dimensional flow over a body (plus displacement surface) with no plane of symmetry.  A 10° half angle cone model with a laminar boundary layer was chosen as the starting point for this effort since convenient simplification is obtained in the equations of motion; and, equally important, very accurate solutions were available in tabular form of the three-dimensional inviscid flow.

In this brief paper, no details of the numerical techniques will be given.  Instead, results of the computations and comparison with

7

experimental data will be discussed. The details of the numerical techniques used may be found in references 1, 2, 3, and 4.

The sequence of the computations which must be run in order to compute the Magnus force is indicated in Figures 3a and 3b. Each block indicates a separate computer program along with its required input information and the output. The two main programs are outlined in asterisks. In order to start the boundary layer computation for the spinning model, initial profile data are generated for the limiting case of the boundary layer at the tip of a non-spinning cone. These data, along with the outer boundary condition of the inviscid flow, enable the marching technique to begin for specific conditions of Mach number, angle-of-attack, wall temperature, spin rate, and free stream properties. The output of this program consists of wall shear and centrifugal pressure gradient contributions to the Magnus effect (these will be discussed in more detail later) and the longitudinal and circum-ferential components of the boundary-layer displacement surface as functions of longitudinal and azimuthal position over the entire surface of the model.

The three-dimensional boundary-layer displacement surface is not merely the vector sum of the two components. A partial differential equation, as derived by Moore[5], must be integrated to yield the proper displacement thickness. Up to this point, the computations have been accomplished in surface coordinates. The inviscid flow program was written using a cylindrical coordinate system to facilitate computations for arbitrary body shapes. As shown in Figure 3b, a separate program performs the transformation to the cylindrical coordinate system and

1. H. A. Dwyer and B. R. Sanders, "Magnus Forces on Spinning Supersonic Cones. Part I: The Boundary Layer," AIAA Paper No. 75-193, AIAA 13th Aerospace Sciences Meeting, Pasadena, California, 20-22 January 1975.

2. H. A. Dwyer, "Three-Dimensional Flow Studies Over a Spinning Cone at Angle of Attack," BRL Contract Report No. 137, U.S. Army Ballistic Research Laboratories, Aberdeen Proving Ground, Maryland, February 1974. AD# 774795.

3. B. R. Sanders, "Three-Dimensional Steady, Inviscid Flow Field Calculations with Application to the Magnus Problem," PhD Dissertation, University of California, Davis, California, May 1974.

4. H. A. Dwyer and B. R. Sanders, "Magnus Forces on Spinning Super-sonic Cones. Part I: The Boundary Layer," to be published as BRL Contract Report, U.S. Army Ballistic Research Laboratories, Aberdeen Proving Ground, Maryland.

5. F. N. Moore, "Displacement Effect of a Three-Dimensional Boundary Layer," NACA TN 2722, June 1952.

8

computes the surface derivatives that define the model plus three-dimensional boundary-layer displacement thickness.

The final step is to compute the inviscid flow over the newly defined body which is an arbitrary configuration with no plane of symmetry. The numerical technique is a shock capturing finite-difference approach using MacCormack's scheme. This method has been successfully used for space shuttle flow field computations[6]. The starting conditions consist of the inviscid flow field for the original model (no boundary-layer displacement surface).

Examples of the circumferential velocity profiles are shown in Figure 4. In this figure, the asymmetric interaction of the surface spin with the inviscid cross flow is clearly indicated. The cross-over from a positive to a negative circumferential velocity required special attention in the numerical differencing technique.

The profile of the three dimensional boundary-layer displacement thickness is shown in Figure 5 for different values of spin rate. The profile for zero spin is symmetric about $\phi = 180°$; while the profiles for $\omega > 0$ are asymmetric. It is interesting that one effect of surface spin is to reduce the maximum thickness of the boundary layer. Also, it is seen that the boundary layer is more thick where the surface spin opposes the cross flow velocity than on the opposite position where surface spin and inviscid cross flow velocity are in the same direction.

The component of the Magnus force resulting from $\tau_x = \mu \ (\partial u/\partial y)_{y=0}$ due to asymmetry in the u velocity profiles is illustrated schematically in Figure 6. Figure 7 illustrates a similar contribution from $\tau_\phi = \mu \ (\partial w/\partial y)_{y=0}$. Figure 8 illustrates the origin of the centrifugal pressure gradient component. Since the integral is greater on the right side, $p_2 = p_1 - \Delta p_{1-2} < p_3 = p_1 - \Delta p_{1-3}$.

The relative magnitude of these components of the Magnus force is shown in Figure 9. It is of interest to note that this is the first time that all four of these contributors to the Magnus effect have been computed and compared. Previous analyses have considered only $\delta*$ alone or, which is actually worse, $\delta*$ and $\Delta p$. The net Magnus force is the arithmetic sum of the four contributors. In Figure 10 the computed Magnus force is compared to experimental measurements made using the

6. P. Kutler, R. F. Warming, and H. Lomax, "Computation of Space Shuttle Flowfields Using Noncentered Finite-Difference Schemes," *AIAA Journal*, Vol. 11, No. 2, February 1973, pp. 196-204.

strain-gage balance technique[7] for two boundary-layer configurations. Considering the small magnitude of the Magnus force, the agreement with experiment is considered to be very encouraging.

### III.   THREE-DIMENSIONAL FLOW MEASUREMENTS

Experimental studies are being carried out to provide data that will be useful in evaluating and help guide the development of the theoretical effort.  The experimental studies consist of:  (1) strain-gage balance force measurements for different boundary-layer configurations;  (2) optical studies of the effects of spin and yaw on boundary-layer transition;  (3) detailed profile measurements of the boundary layer on a yawed, spinning body of revolution; and (4) wall static pressure measurements on a yawed body of revolution.

The profile measurements are being made on a tangent-ogive-cylinder model that has a one caliber ogive section and an overall length of seven calibers.  Measurements have been made for M = 3, $\alpha = 4°$, and spin rates of 0 and 10,000 RPM.  The model as installed in the tunnel with the total head probe and survey mechanism is shown in Figure 11.  Measurements have been made at 30° increments in azimuth completely about the circumference of the model.  An example of some measured velocity profiles for a tripped turbulent boundary layer is shown in Figure 12.  These measurements were made at an axial position 6.0 calibers from the tip of the model.  The velocities were computed from total pressure surveys of the boundary layer assuming a constant total temperature through the boundary layer equal to the tunnel total temperature and a constant static pressure across the boundary layer equal to the wall pressure measured as described below.

Measurements are being made of the wall static pressure on slender bodies of revolution to enable velocity profiles to be computed from the total head surveys, and also for comparison with computations made using the inviscid flow computer program.  Examples of these data are shown in Figures 13 and 14.  These data were obtained on a tangent-ogive-cylinder model identical to the model used for the profile measurements.  These data indicate that the wall pressure is well behaved for $\alpha \leqslant 4°$; however, as $\alpha$ increases to 6° and 10°, the effect of vortex formation on the inviscid pressure field is evident.

---

7.   W. B. Sturek, "Boundary Layer Studies on a Spinning Cone," BRL Report No. 1649, U.S. Army Ballistic Research Laboratories, Aberdeen Proving Ground, Maryland, May 1973.  AD 762564.  Also, "Boundary-Layer Distortion on a Spinning Cone," AIAA Journal, Vol. 11, No. 3, March 1973, pp. 395-396.

# IV. PLANS FOR FUTURE RESEARCH

Effort is underway to extend the capabilities of the boundary layer computer program to include the effects of axial pressure gradient and turbulence. These capabilities are essential in order for the computation techniques to be of value in the design of artillery projectiles.

Additional experiments are planned to obtain boundary layer profile data (including turbulence measurements), wall static pressure, and force measurements for additional slender bodies of revolution including a boattail afterbody.

## REFERENCES

1. H. A. Dwyer and B. R. Sanders, "Magnus Forces on Spinning Super-
   sonic Cones. Part I: The Boundary Layer," AIAA Paper No. 75-193,
   AIAA 13th Aerospace Sciences Meeting, Pasadena, California, 20-22
   January 1975.

2. H. A. Dwyer, "Three-Dimensional Flow Studies Over a Spinning Cone
   at Angle of Attack," BRL Contract Report No. 137, U.S. Army
   Ballistic Research Laboratories, Aberdeen Proving Ground, Maryland,
   February 1974. AD# 774795.

3. B. R. Sanders, "Three-Dimensional, Steady, Inviscid Flow Field
   Calculations with Application to the Magnus Problem," PhD
   Dissertation, University of California, Davis, California, May
   1974.

4. H. A. Dwyer and B. R. Sanders, "Magnus Forces on Spinning Super-
   sonic Cones. Part I: The Boundary Layer," to be published as a
   BRL Contract Report, U.S. Army Ballistic Research Laboratories,
   Aberdeen Proving Ground, Maryland.

5. F. N. Moore, "Displacement Effect of a Three-Dimensional Boundary
   Layer," NACA TN 2722, June 1952.

6. P. Kutler, R. F. Warming, and H. Lomax, "Computation of Space
   Shuttle Flowfields Using Noncentered Finite-Difference Schemes,"
   *AIAA Journal*, Vol. 11, No. 2, February 1973, pp. 196-204.

7. W. B. Sturek, "Boundary Layer Studies on a Spinning Cone," BRL
   Report No. 1649, U.S. Army Ballistic Research Laboratories,
   Aberdeen Proving Ground, Maryland, May 1973. AD 762564.
   Also, "Boundary-Layer Distortion on a Spinning Cone," *AIAA Journal*,
   Vol. 11, No. 3, March 1973, pp. 395-396.
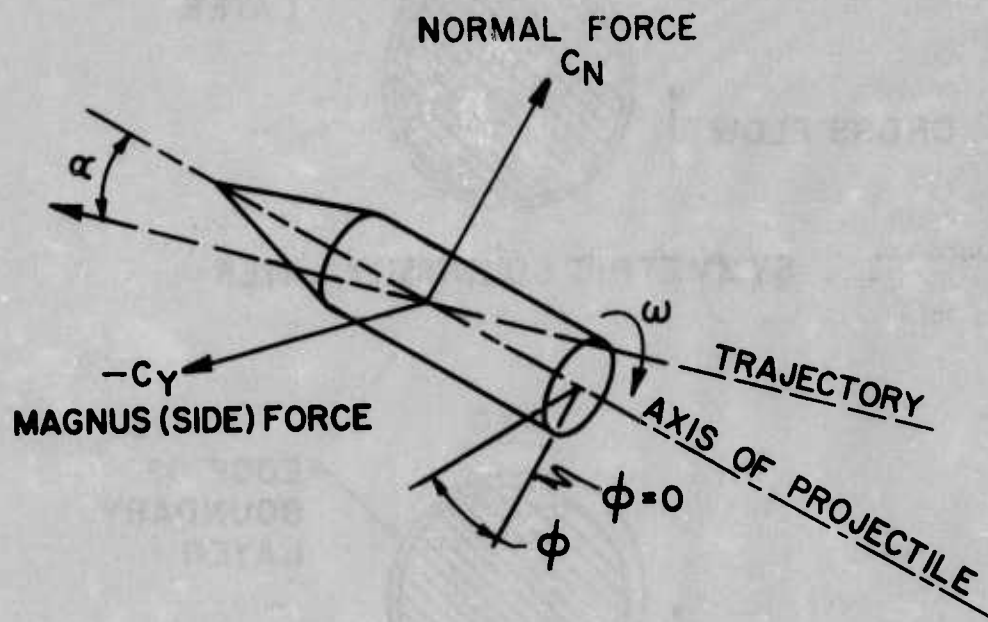
Figure 1. Magnus Force on Spinning Projectile

13
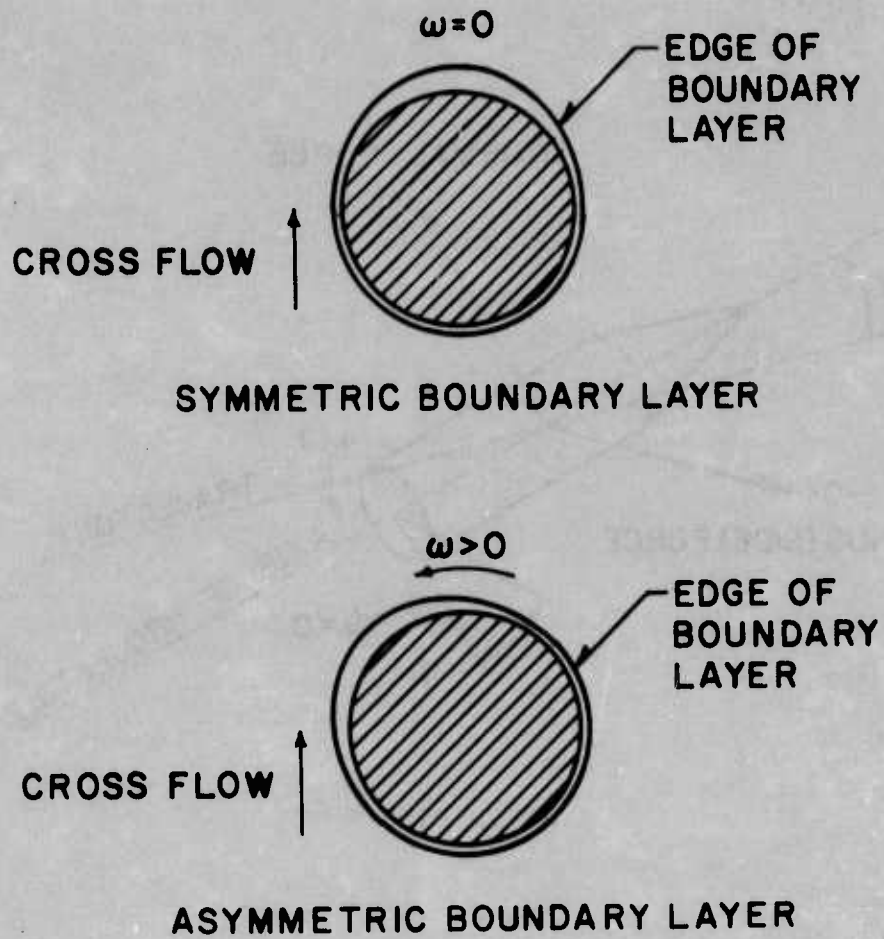
Figure 2.   Schematic Cross-Sectional View of a Body at Angle of Attack
Showing Distortion of the Boundary Layer by Spin

14
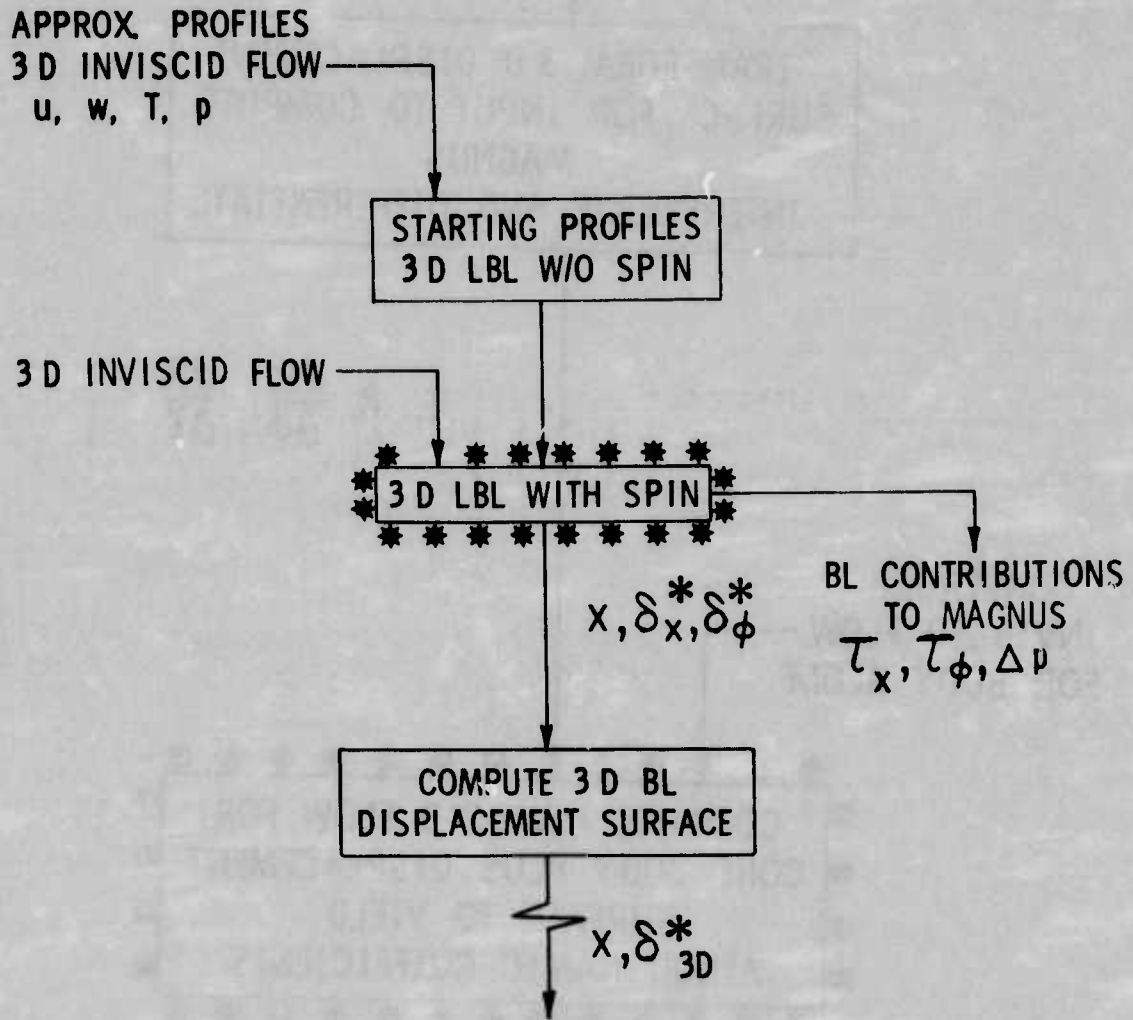
Figure 3a. Sequence of Computations, Surface Coordinates

15

$X, \delta^*_{3D}$

```
┌─────────────────────────────┐
│   TRANSFORM 3D DISPLACEMENT  │
│  SURFACE FOR INPUT TO COMPUTE│
│            MAGNUS            │
│  INTERPOLATE AND DIFFERENTIATE│
└─────────────────────────────┘
```

$Z, \; R, \; \dfrac{\partial R}{\partial \phi}, \; \dfrac{\partial R}{\partial Z}$

CONVERGED
INVISCID FLOW
FOR BODY ALONE

```
┌─────────────────────────────┐
│   COMPUTE INVISCID FLOW FOR  │
│  CONE BODY PLUS DISPLACEMENT │
│        SURFACE TO YIELD      │
│   AERODYNAMIC COEFFICIENTS   │
└─────────────────────────────┘
```

$C_Y, \; C_{YM}, \; C_N, \; C_M$
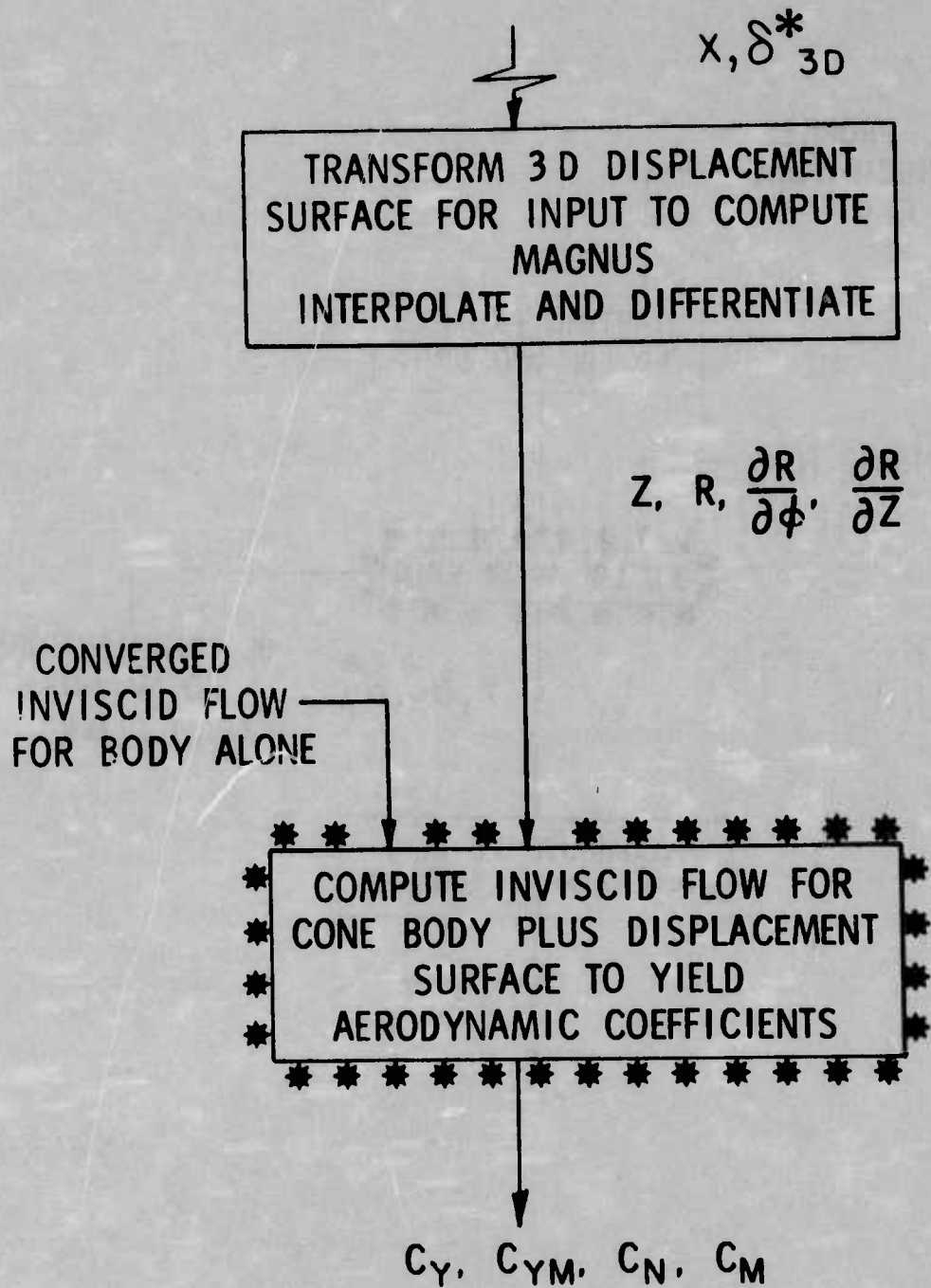
Figure 3b.   Sequence of Computations, Cylindrical Coordinates

16
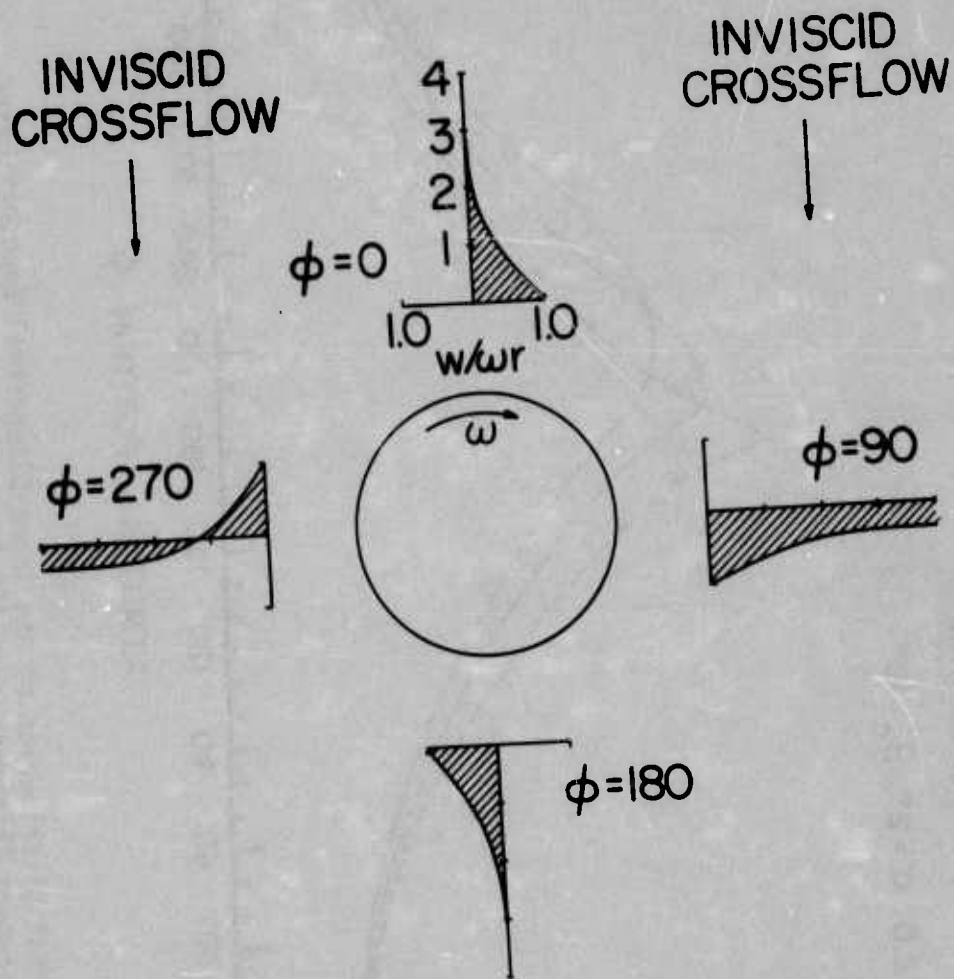
Figure 4.  Circumferential Velocity Profiles for Laminar Boundary Layer, 10° Cone Model, M = 2, $\alpha$ = 1°, $\omega$ = 10,000 RPM

17
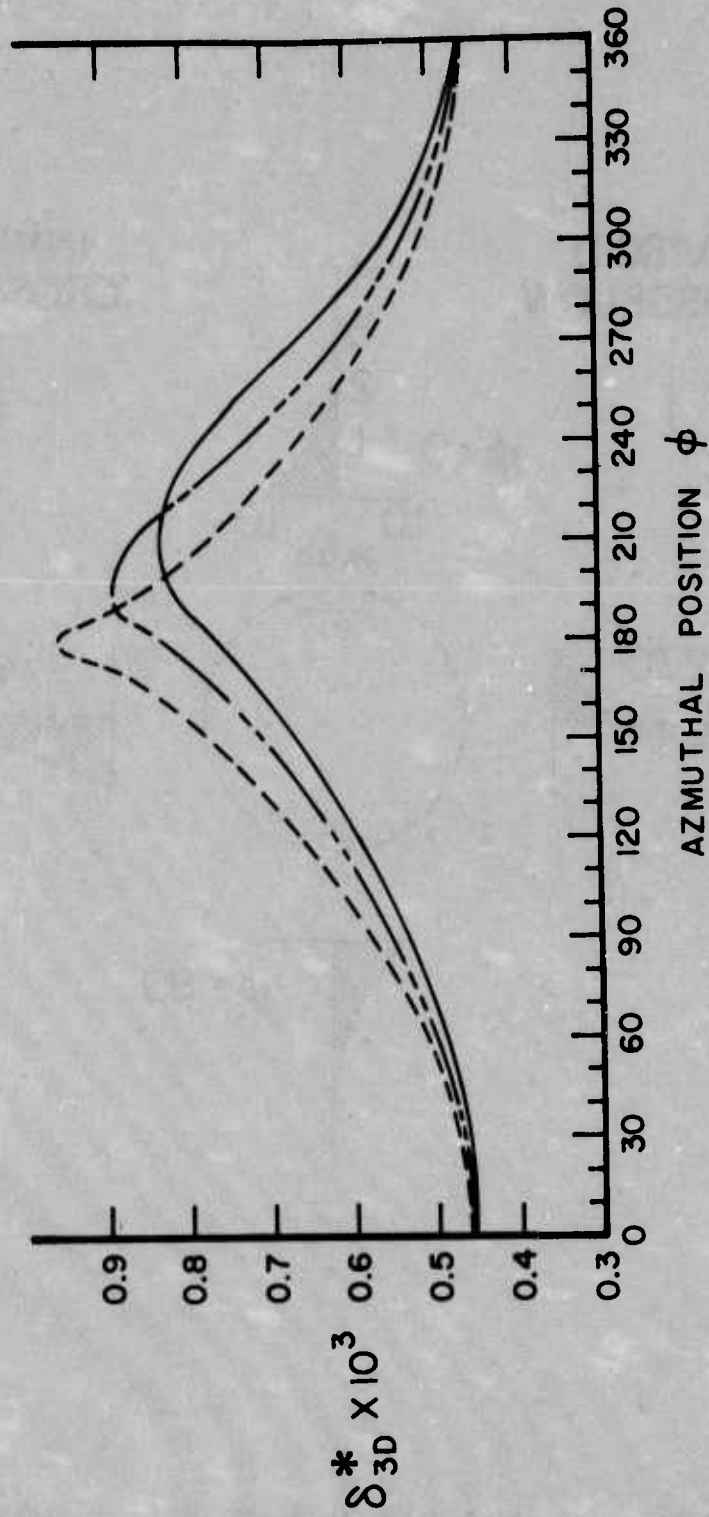
Figure 5. Azimuthal Distribution of the Three-Dimensional Boundary-Layer Displacement Thickness on a 10° Cone Model (X/L = .886)
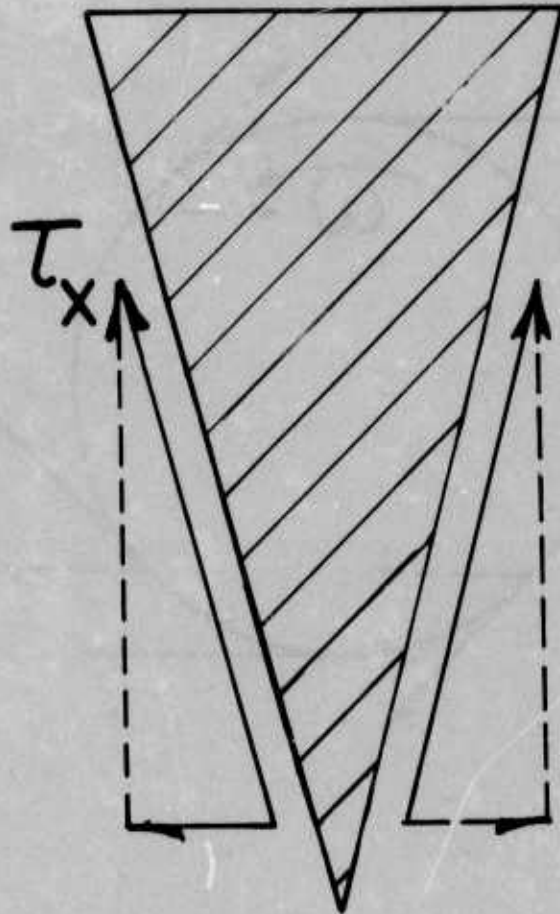
Figure 6. Schematic Illustration of the Longitudinal Velocity
Component of Wall Shear Stress for a Cone Model

19
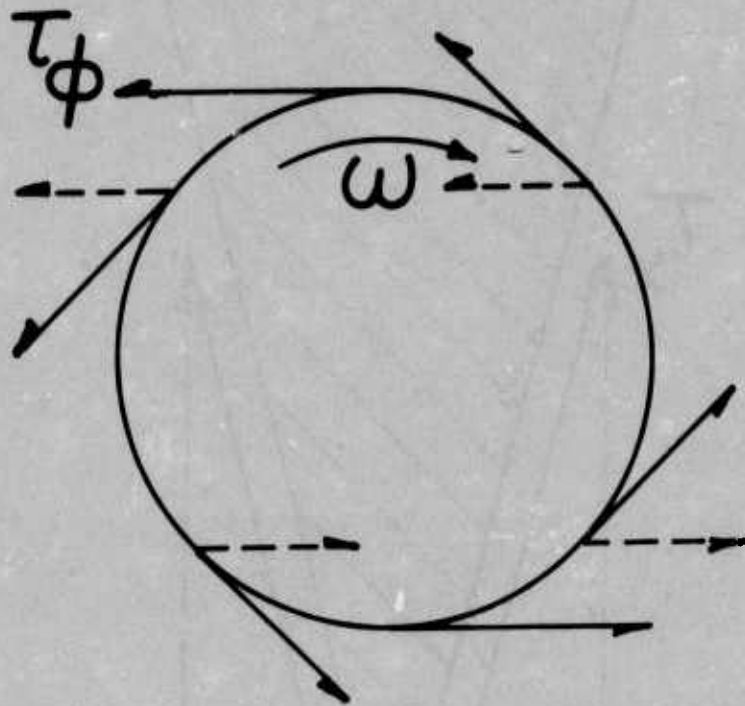
Figure 7. Schematic Illustration of the Circumferential Velocity Component of Wall Shear Stress for a Spinning Body of Revolution

20

INVISCID CROSSFLOW VELOCITY, $W_\infty$
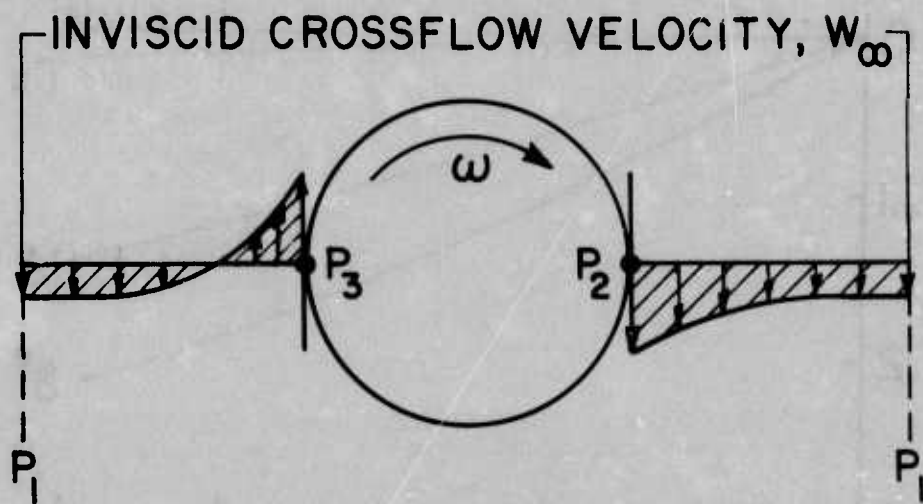
$$\Delta p = \int_0^\delta \rho \frac{W^2}{R} \, dy$$

Figure 8. Schematic Illustration of the Centrifugal Pressure
Gradient Contribution to a Side Force With
Superimposed Cross Flow Velocity Profiles

21
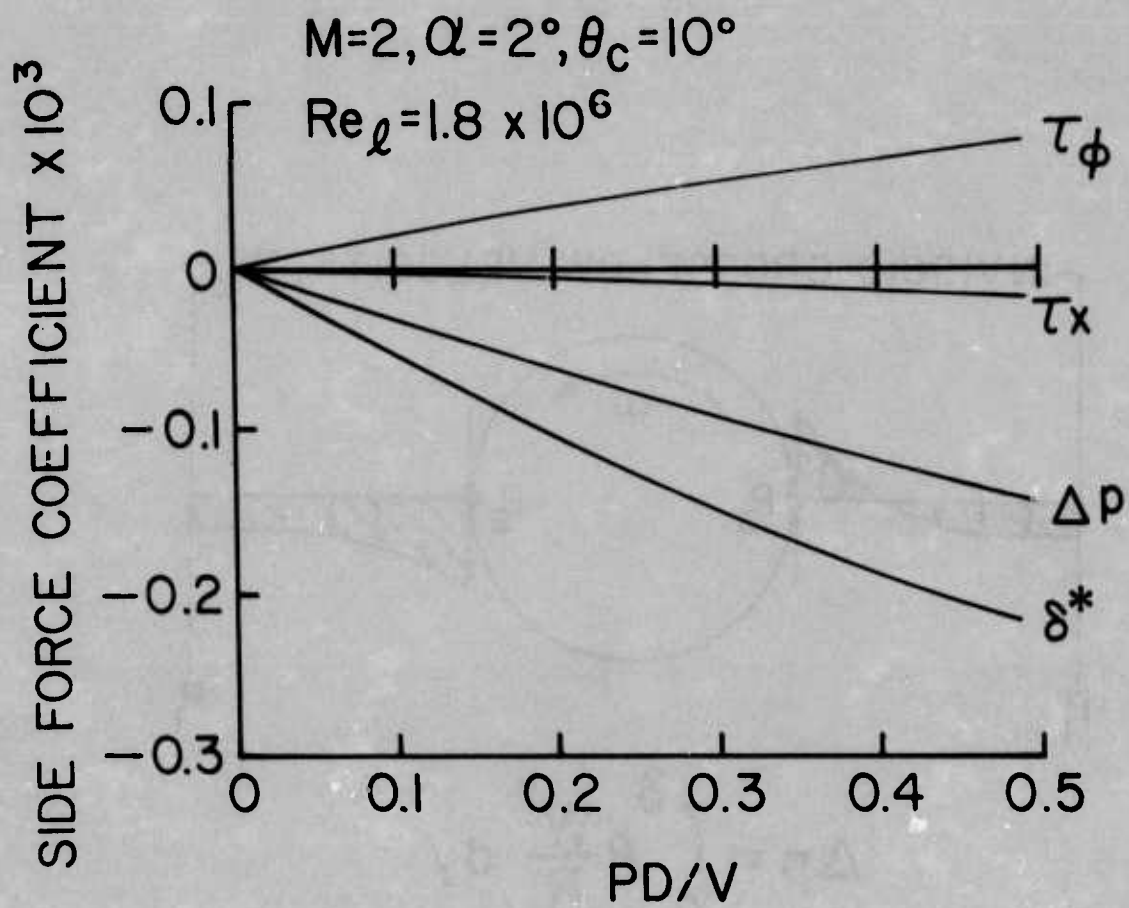
Figure 9.  Comparison of Computed Values for the
Four Contributors to the Magnus Force

22
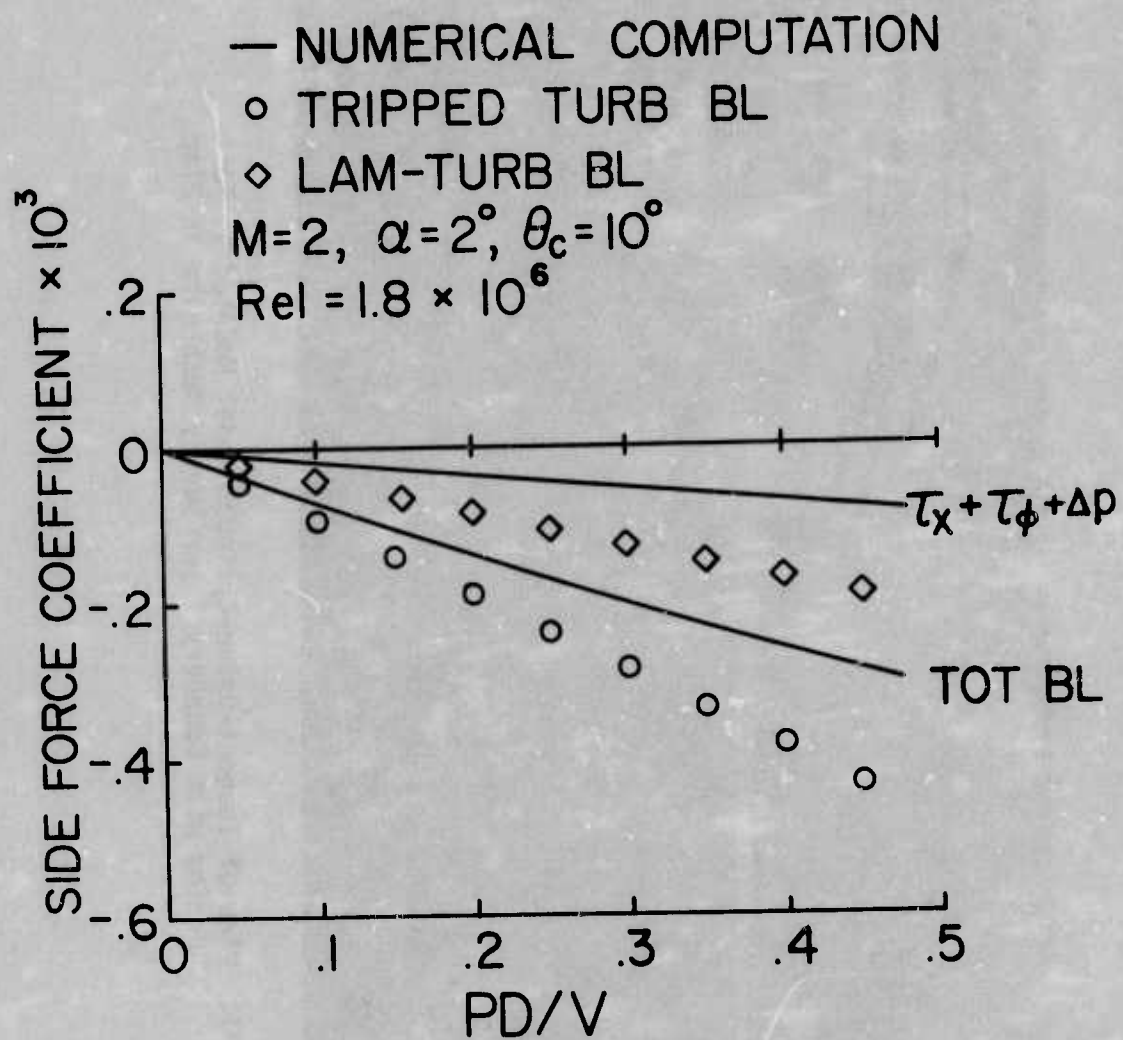
Figure 10. Comparison of Computed Values of Magnus Force to Experimental Measurements for Two Boundary Layer Configurations

23
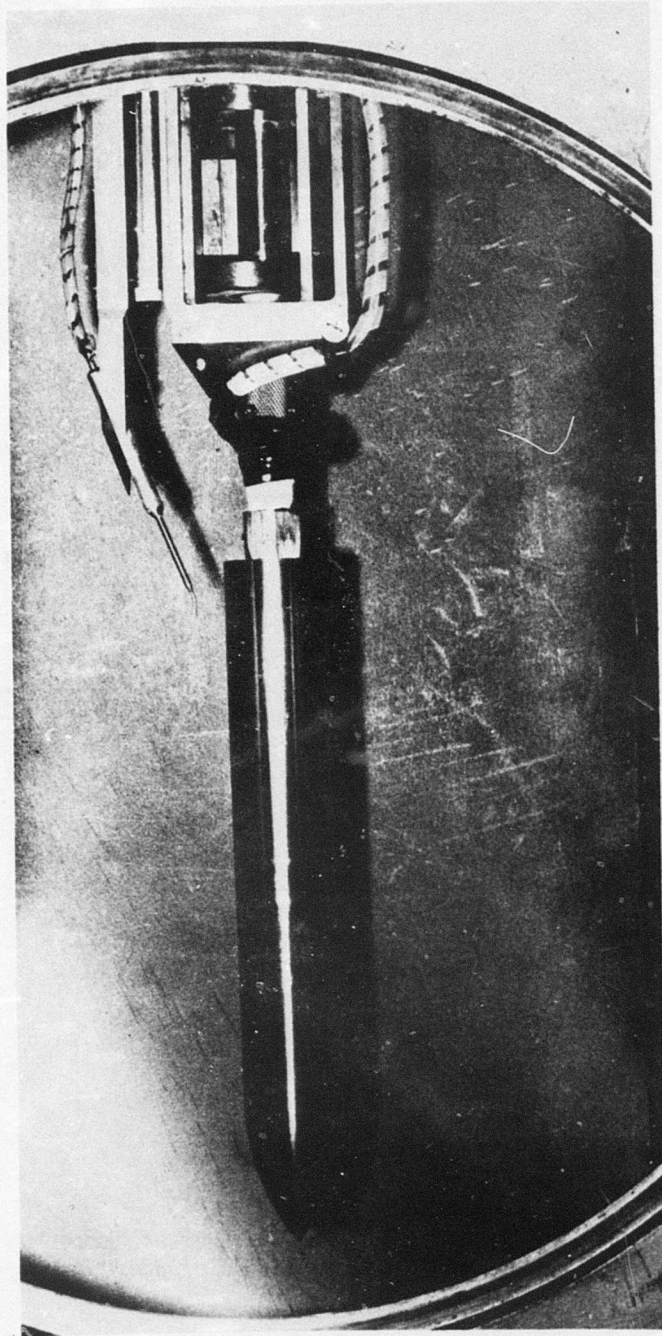
Figure 11. View of Tangent-Ogive-Cylinder Model Mounted in Test Section with Boundary Layer Survey Mechanism in Place
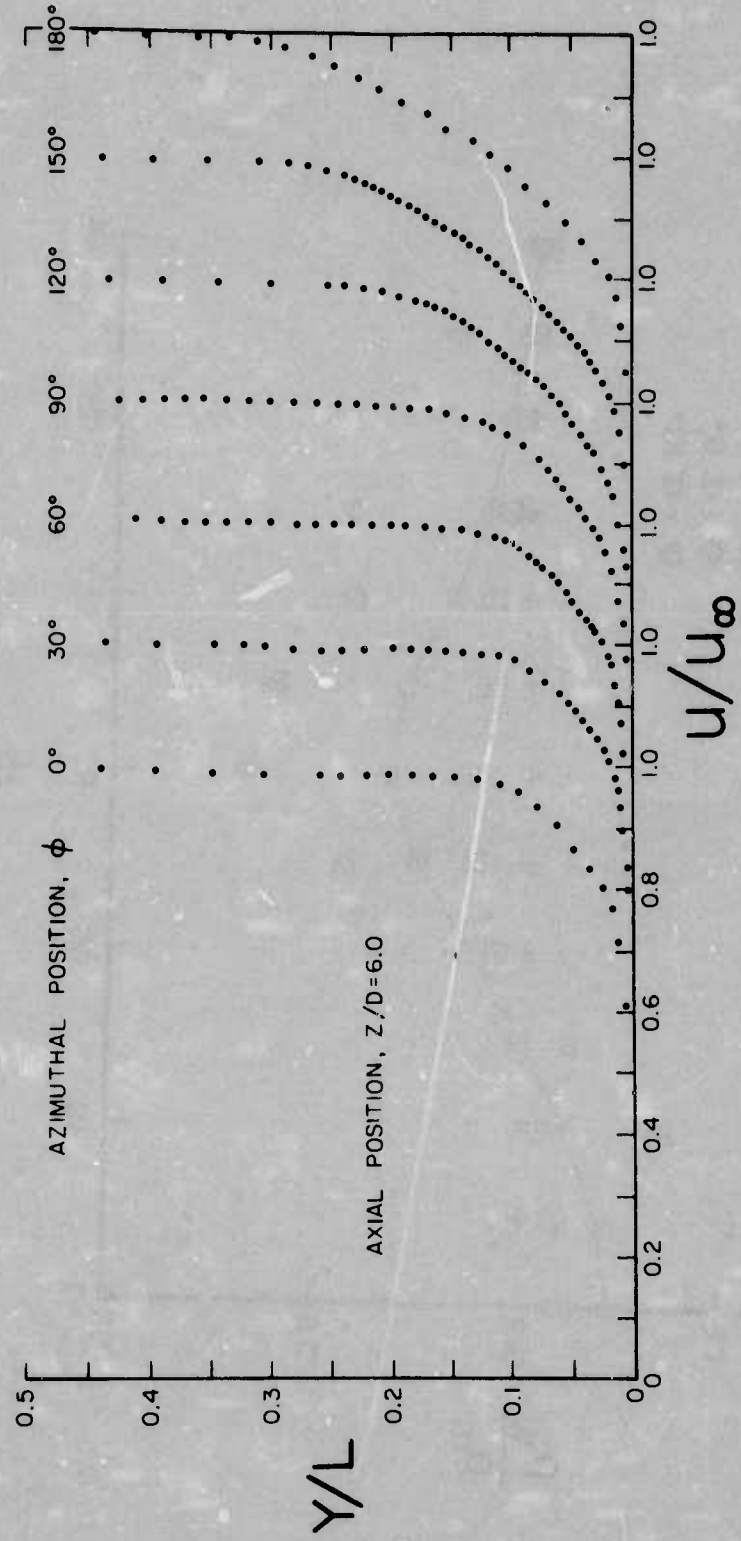
Figure 12. Velocity Profiles of the Tripped Turbulent Boundary Layer on the Tangent-Ogive-Cylinder Model at $Z/D = 6.0$, $M = 3$, $\alpha = 4°$, $\omega = 0$ RPM ($L = 2.54$ cm)

25
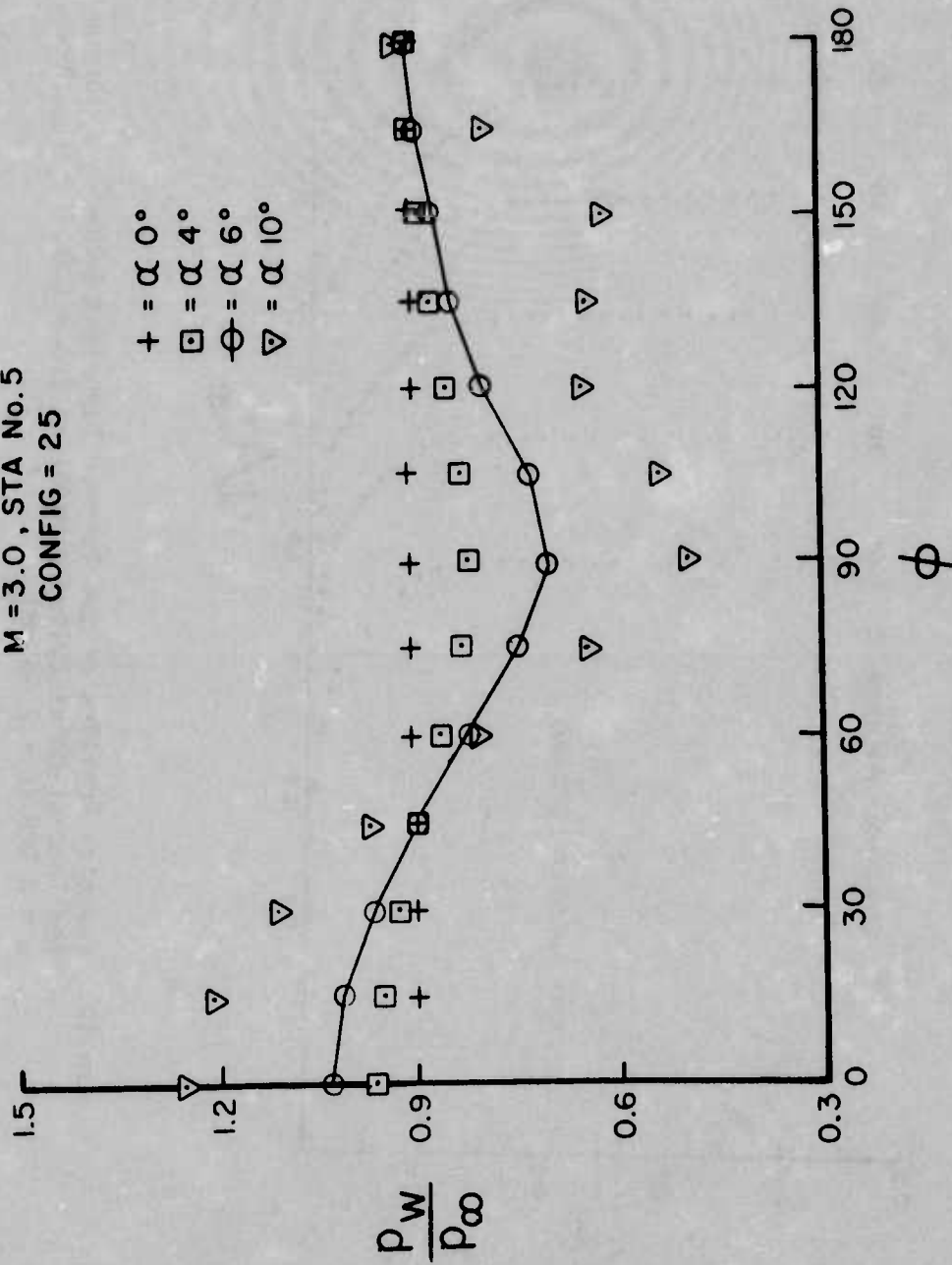
Figure 13. Azimuthal Variation of Wall Static Pressure on the Tangent-Ogive-Cylinder Model for Different Angles of Attack, $M = 3$, $Z/D = 4.5$

26
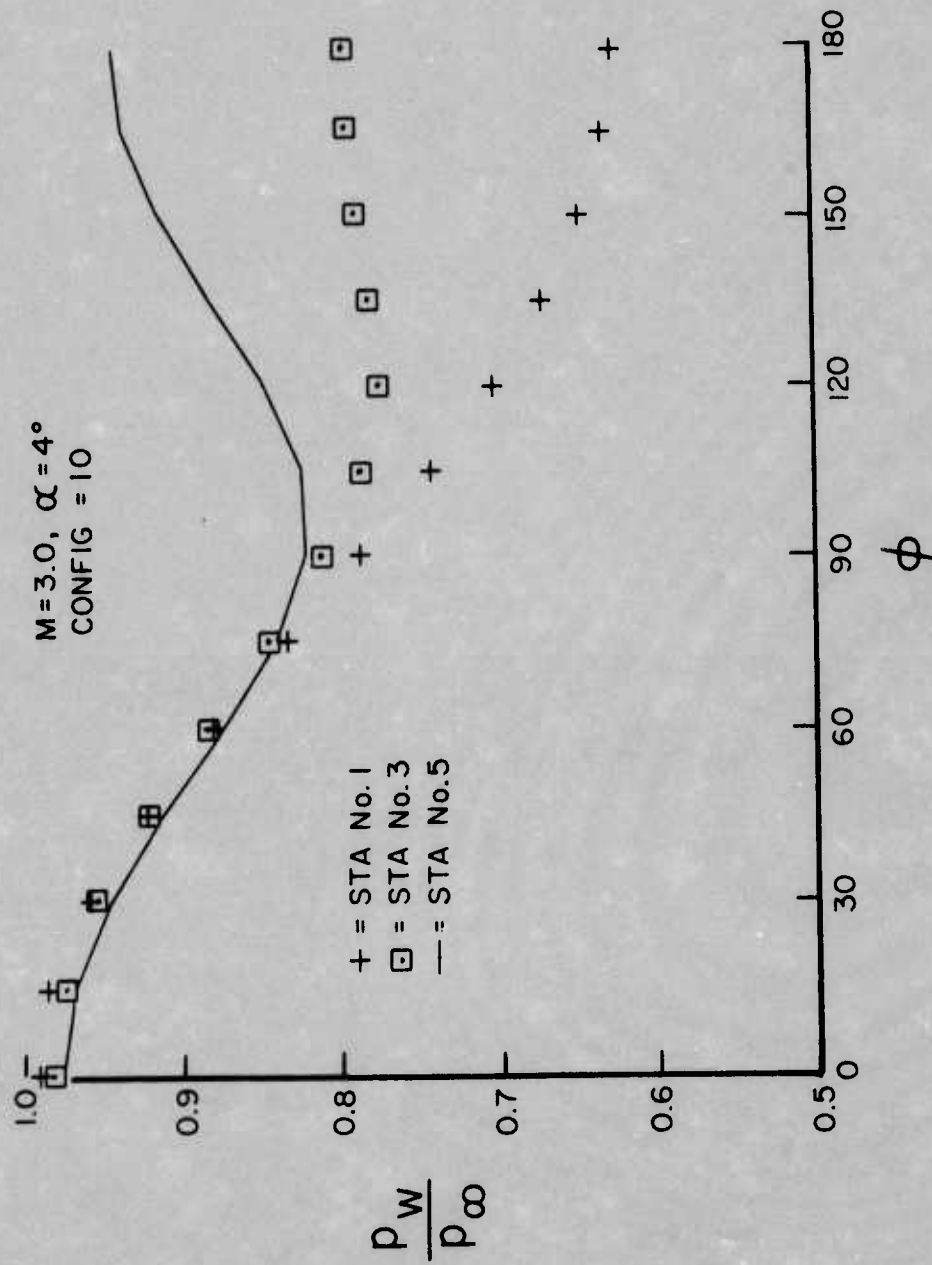
Figure 14. Azimuthal Variation of Wall Static Pressure on the Tangent-Ogive-Cylinder Model for Different Axial Positions, M = 3, α = 4°, Sta 1: Z/D = 1.25, Sta 3: Z/D = 2.5, Sta 5: Z/D = 4.5

27

## LIST OF SYMBOLS

$C_N$      normal force coefficient

$C_M$      pitching moment coefficient

$C_Y$      Magnus force coefficient

$C_{YM}$      Magnus moment coefficient

$D$      diameter of base of model

$L$      reference length, 30.48 cm

$M$      Mach number

$P$      spin rate, radians per second

$p_{t_2}$      total pressure behind a normal shock wave, measured using the total head probe

$p_w$      wall static pressure

$p_\infty$      tunnel free stream static pressure

$R$      distance from axis of cone to the outer edge of the cone plus three-dimensional boundary-layer displacement thickness

$Re_\ell$      Reynolds number based tunnel free stream properties and length of model

$r$      local radius of cone

$u$      velocity in X direction

$V$      tunnel free stream velocity

$w$      circumferential component of velocity

$X$      longitudinal surface coordinate

$y$      coordinate perpendicular to the local surface

$z$      axial coordinate

## LIST OF SYMBOLS (Continued)

$\delta^*$      boundary-layer displacement thickness, also used to signify the boundary-layer displacement thickness contribution to the Magnus force

$\Delta p$      centrifugal pressure gradient contribution to the Magnus force

$\theta_c$      cone half angle

$\tau_x$      longitudinal velocity component of wall shear stress; also used to signify the longitudinal velocity component of wall shear stress contribution to the Magnus force

$\tau_\phi$      circumferential velocity component of wall shear stress; also used to signify the circumferential velocity component of wall shear stress contribution to the Magnus force

$\phi$      azimuthal position, $\phi = 0$ is wind side

$\omega$      spin rate, RPM

## DISTRIBUTION LIST

| No. of Copies | Organization |
|---|---|
| 2 | Commander<br>Defense Documentation Center<br>ATTN: DDC-TCA<br>Cameron Station<br>Alexandria, VA 22314 |
| 1 | Commander<br>US Army Materiel Command<br>ATTN: AMCDMA-ST<br>5001 Eisenhower Avenue<br>Alexandria, VA 22333 |
| 1 | Commander<br>US Army Materiel Command<br>ATTN: AMCRD-R<br>5001 Eisenhower Avenue<br>Alexandria, VA 22333 |
| 1 | Commander<br>US Army Materiel Command<br>ATTN: AMCRD-T<br>5001 Eisenhower Avenue<br>Alexandria, VA 22333 |
| 1 | Commander<br>US Army Materiel Command<br>ATTN: AMCRD-A<br>5001 Eisenhower Avenue<br>Alexandria, VA 22333 |
| 1 | Commander<br>US Army Aviation Systems<br>Command<br>ATTN: AMSAV-E<br>12th and Spruce Streets<br>St. Louis, MO 63166 |
| 1 | Director<br>US Army Air Mobility Research<br>and Development Laboratory<br>Ames Research Center<br>Moffett Field, CA 94035 |

| No. of Copies | Organization |
|---|---|
| 1 | Commander<br>US Army Electronics Command<br>ATTN: AMSEL-RD<br>Fort Monmouth, NJ 07703 |
| 1 | Commander<br>US Army Jefferson Proving<br>Ground<br>ATTN: STEJP-TD-D<br>Madison, IN 47250 |
| 4 | Commander<br>US Army Missile Command<br>ATTN: AMSMI-R<br>AMSMI-RDK<br>Mr. R. Deep<br>Mr. R. Becht<br>Dr. D. Spring<br>Redstone Arsenal, AL 35809 |
| 2 | Commander<br>US Army Mobility Equipment<br>Research & Development Center<br>ATTN: Tech Docu Ctr, Bldg 315<br>AMSME-RZT<br>Fort Belvoir, VA 22060 |
| 1 | Commander<br>US Army Tank Automotive<br>Logistics Command<br>ATTN: AMSTA-RHFL<br>Warren, MI 48090 |
| 1 | Commander<br>US Army Armament Command<br>Rock Island, IL 61202 |
| 3 | Commander<br>US Army Picatinny Arsenal<br>ATTN: SARPA-FR-S-A<br>Mr. A. Loeb<br>Mr. D. Mertz<br>Mr. E. Falkowski<br>Dover, NJ 07801 |

DISTRIBUTION LIST

| No. of Copies | Organization | No. of Copies | Organization |
|---|---|---|---|
| 1 | Commander<br>US Army Harry Diamond Labs.<br>ATTN: AMXDO-TI<br>2800 Powder Mill Road<br>Adelphi, MD 20783 | 1 | Douglas Aircraft Company<br>McDonnell-Douglas Corp.<br>ATTN: Dr. Tuncer Cebeci<br>3855 Lakewood Boulevard<br>Long Beach, CA 90801 |
| 1 | Director<br>US Army TRADOC Systems<br>Analysis Activity<br>ATTN: ATAA-SA<br>White Sands Missile Range<br>NM 88002 | 1 | Sandia Laboratories<br>ATTN: Dr. F. G. Blottner<br>P.O. Box 5800<br>Albuquerque, NM 87115 |
| 1 | Commander<br>US Army Research Office<br>P.O. Box 12211<br>Research Triangle Park, NC 27709 | 1 | Princeton University<br>James Forrestal Research Center<br>Gas Dynamics Laboratory<br>ATTN: Prof. S. Bogdonoff<br>Princeton, NJ 08540 |
| 1 | Commander<br>David W. Taylor Naval Ship<br>Research & Development Center<br>ATTN: Dr. S. de los Santos<br>Aerodynamics Lab<br>Bethesda, MD 20084 | 1 | University of California<br>Department of Mechanical<br>Engineering<br>ATTN: Prof. H. A. Dwyer<br>Davis, CA 95616 |
| 4 | Commander<br>US Naval Surface Weapons Center<br>ATTN: Code 312, Mr. S. Hastings<br>Code 313, Mr. R. Lee<br>Mr. W. Yanta<br>Mr. R. Voisinet<br>Silver Spring, MD 20910 | 1 | University of Delaware<br>Mechanical and Aerospace<br>Engineering Department<br>ATTN: Dr. J. E. Danberg<br>Newark, DE 19711 |
| 1 | Commander<br>US Naval Surface Weapons Center<br>ATTN: Dr. W. Kemper<br>Dahlgren, VA 22448 | 1 | University of Virginia<br>Department of Aerospace<br>Engineering and Engineering<br>Physics<br>ATTN: Prof. I. Jacobson<br>Charlottesville, VA 22904 |
| 2 | Director<br>National Aeronautics and<br>Space Administration<br>Langley Research Center<br>ATTN: MS 185, Tech Library<br>MS 161, Mr. D. Bushnell<br>Langley Station<br>Hampton, VA 23365 | | |

Aberdeen Proving Ground

Marine Corps Ln Ofc
Director, USAMSAA